Analysis of the high resolution absorption spectrum of ethylene between 5800 and 6400 cm–1

O. Ben Fathallah, Michael M. Rey, A. Campargue

Journal of Quantitative Spectroscopy & Radiative Transfer 316 (2024) 108905

Contents lists available at ScienceDirect

Journal of Quantitative Spectroscopy and Radiative Transfer

journal homepage: www.elsevier.com/locate/jqsrt

Analysis of the high resolution absorption spectrum of ethylene between 5800 and 6400 cm^{-1}

O. Ben Fathallah [a,b], M. Rey [c], A. Campargue [a,*]

[a] Univ. Grenoble Alpes, CNRS, LIPhy, 38000 Grenoble, France
[b] Laboratoire de Spectroscopie et Dynamique Moléculaire, Ecole Nationale Supérieure d'Ingénieurs de Tunis, Université de Tunis, 5 Av Taha Hussein 1008 Tunis, Tunisia
[c] GSMA, UMR CNRS 7331, University of Reims Champagne Ardenne, Moulin de la Housse B.P. 1039, Cedex Reims F-51687, France

ARTICLE INFO

Keywords:
Ethylene
Ethene
C_2H_4
Rovibrational assignments
Variational calculations

ABSTRACT

The highly congested room temperature absorption spectrum of ethylene (C_2H_4) is analyzed in the range 5800–6400 cm^{-1} on the basis of a previously elaborated empirical list of more than 12,200 lines. The investigated spectral interval coincides to a region of weak absorption of water, methane and acetylene. Quantitative information on the relatively strong C_2H_4 absorption in the region is valuable for trace detection applications.

Relying on the position and intensity agreement with a line list of $^{12}C_2H_4$ transitions calculated by the variational method, 1674 transitions could be assigned to five bands ($\nu_5+\nu_9$, $\nu_5+\nu_{11}$, $\nu_2+\nu_3+\nu_{11}$, $\nu_2+\nu_6+\nu_9$ and $\nu_1+\nu_{11}$). All the reported assignments are confirmed by Lower State Combination Difference (LSCD) relations *i.e.* all the upper states (607 in total) have coinciding determinations of their energies through several transitions (up to 6). The position and intensity comparisons between experiment and theory are discussed together with a comparison to previous works in the region.

1. Introduction

The present contribution aims at providing new quantitative laboratory data on the absorption spectrum of ethylene which are essential for reliable remote sensing. Indeed, there is a lack of high resolution data in the current spectroscopic databases. For instance, the HITRAN database [1] provides line parameters for only two spectral intervals, 620–1530 cm^{-1} and 2929–3242 cm^{-1}, the latter corresponding to the fundamental CH stretching modes. The first overtone of the CH stretching manifold (ΔV_{CH}= 2) near 1.6 μm is favorable for trace detection as it provides a good compromise between the intensity of the transitions of the molecule to be detected and the performances of the optical devices in the region. Interestingly, the $\nu_5+\nu_9$ stretching band of ethylene which dominates the ΔV_{CH}= 2 absorption region is significantly shifted towards higher energies, compared to the $2\nu_3$ stretching band which dominates the ΔV_{CH}= 2 absorption region of methane (centers around 6150 and 6000 cm^{-1}, respectively). The 1.6 μm region coinciding to an important transparency window in our atmosphere, it makes the $\nu_5+\nu_9$ band particularly suitable for quantitative detection of ethylene even when the analyzed gas mixture includes a significant amount of methane (see for instance Fig. 2 in Ref. [2]). Different photoacoustic detection schemes using laser diodes have been proposed for the detection of ethylene in the 1.6 μm region with targeted detectivity threshold in the tens-ppb range [2,3].

The literature review indicates that extensive spectra of ethylene near 1.6 μm were recorded at high resolution with a variety of experimental approaches: *(i)* Bach et al. used Fourier transform spectroscopy (FTS) both at room temperature and low rotational temperature (53 K) in a slit-jet expansion [4], *(ii)* Platz and Demtroder reported an FTS spectrum at room temperature between 6070 and 6230 cm^{-1} together with a sub-Doppler spectrum obtained in a molecular beam with an optothermal detection near the $\nu_5+\nu_9$ band center (6147 - 6170 cm^{-1}) [5], *(iii)* two-channel photo-acoustic spectra were reported with absolute cross section values over the wide 6035.5- 6207.5 cm^{-1} region, by Kapitanov and Ponomarev [6], *(iv)* Parkes et al. retrieved absolute line intensities of 17 strong ^QQ lines of the $\nu_5+\nu_9$ band from spectra recorded by cavity ring down spectroscopy (CRDS) near 6150 cm^{-1} [7]. To the best of our knowledge, this latter work is the only one where absolute line intensities were reported in the region, *(v)* finally, Loroño Gonzalez et al. [8] assigned 600 experimental lines to the $\nu_5+\nu_9$ and $\nu_5+\nu_{11}$ stretching dyad in their FTS and opto-acoustic spectra and proposed an effective model restricted to the two interacting vibrational bands. No intensity information was provided in that work.

We have recently undertaken a systematic study of the ethylene

* Corresponding author.
E-mail address: alain.campargue@univ-grenoble-alpes.fr (A. Campargue).

https://doi.org/10.1016/j.jqsrt.2024.108905
Received 28 November 2023; Received in revised form 10 January 2024; Accepted 10 January 2024
Available online 12 January 2024

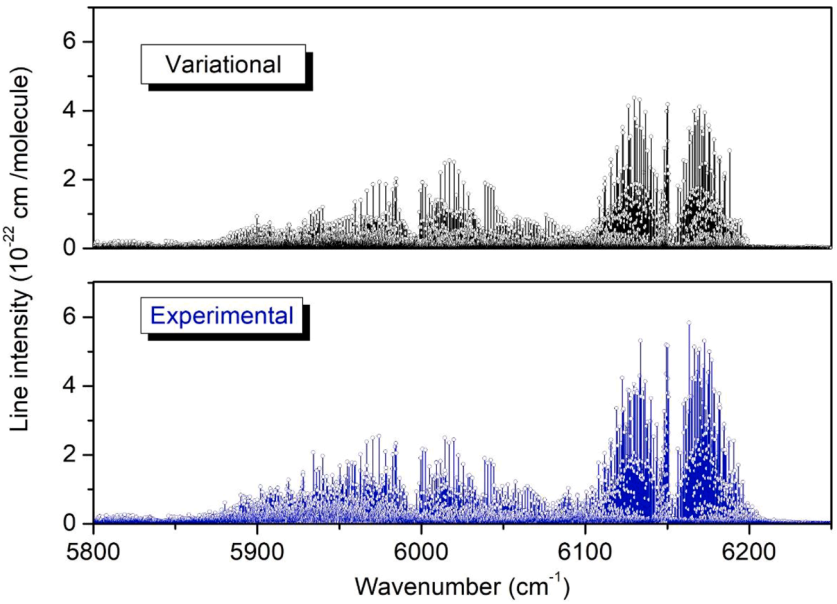

Fig. 1. Overview comparison of the ethylene spectrum at room temperature in the 5800–6250 cm^{-1} interval. The variational line list of Ref. [9] (upper panel) is compared to the FTS line list obtained in Ref. [11] analyzed in the present work. For a proper comparison of these stick spectra, variational doublets have been merged in single transitions with the intensity sum of the two components.

spectrum in the near infrared by Fourier transform spectroscopy [9]. Our investigation includes the elaboration of extensive empirical line lists over wide spectral regions and (when possible) the rovibrational assignments of the transitions by comparison to calculated line lists recently obtained from variational calculations. In a first contribution, we considered FTS ethylene spectra recorded at four temperatures (130, 201, 240 and 297 K) and two pressures in the 6700–7260 cm^{-1} region, thus above the ΔV_{CH}= 2 absorption region [9]. A new theoretical line list based on an accurate *ab initio* potential and dipole moment surfaces and extensive first-principle calculations was generated and used for the assignments [9]. This list extends up to 9000 cm^{-1} the previous room temperature TheoReTS variational list available up to 6400 cm^{-1} [10]. A total of 647 transitions could be rovibrationally assigned to seven vibrational bands observed in an FTS spectrum at 130 K. The assignments based on a reasonable agreement between the measured and calculated positions and intensities were all confirmed by Lower State Combination Difference (LSCD) relations. Note that in the considered region, the deviations of the calculated position from the measured values are typically within ± 3 cm^{-1}.

The aim of the present contribution is to follow a similar procedure for the analysis of the C_2H_4 spectrum in the above discussed 5800–6400 cm^{-1} region which is of more interest for trace detection applications. Although not published, an extensive empirical line list of ethylene has been elaborated in Ref. [11] in this particular region. This list of 12,254 lines with intensity larger than 1×10^{-24} cm/molecule was retrieved from a room temperature ethylene spectrum recorded at Brussels University (ULB) and used in order to identify C_2H_4 lines in a CRDS spectrum of acetylene. Indeed, the acetylene spectrum is extremely weak in

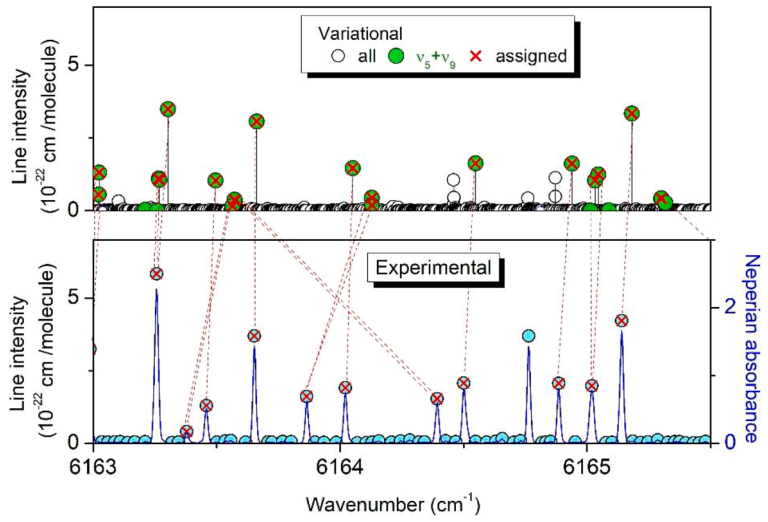

Fig. 2. Rovibrational assignments of the transitions of the $\nu_5 + \nu_9$ band of ethylene near 6164 cm^{-1}.
Upper panel: Variational line list. Open circles correspond to the full calculated line list [9]. Among the calculated transitions of the $\nu_5 + \nu_9$ band (green symbols), those marked by a red cross have been identified in the experimental list.
Lower panel: Experimental spectrum recorded at ULB and corresponding list (cyan dots) [11]. The assigned transitions (red crosses) are linked to their variational counterpart.

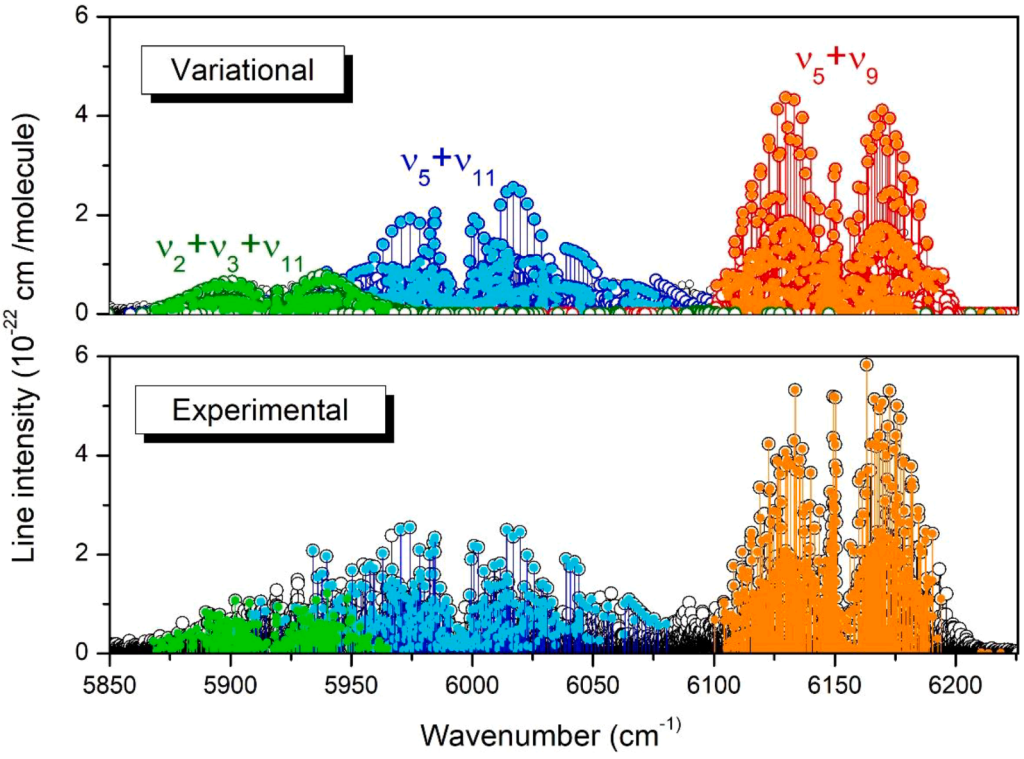

Fig. 3. Overview of the assignments of the transitions of the $\nu_2+\nu_3+\nu_{11}$, $\nu_5+\nu_{11}$ and $\nu_5+\nu_9$ bands of ethylene (green, blue and orange circles, respectively). *Upper panel:* Variational line list [9]. Open and filled circles correspond to the totality and to the assigned transitions of the three bands, respectively. *Lower panel:* Experimental list. The assigned transitions of the three considered bands are highlighted.

the region and a 5 ppm relative abundance of C_2H_4 in the studied acetylene sample is sufficient to make ethylene lines dominate the acetylene spectrum near 6150 cm^{-1} [11].

The remaining part of the paper is organized as follows. In the next section, we describe the assignment process by comparison to the variational line list. In section 3, the level of agreement between experiment and theory will be discussed. The discussion will include a comparison to the (scarce) measured line intensities available in the literature. We will also consider our rovibrational assignments in comparison to those based on an effective Hamiltonian model of two interacting vibrational bands reported by Loroño Gonzalez et al. [8].

2. Rovibrational assignments

2.1. Experimental line list

In Ref. [11], a high resolution (0.011 cm^{-1}) room temperature (294±1 K) FTS spectrum of ethylene was recorded at ULB at a pressure of 0.360(5) Torr. The gas was contained in a 1.72-m long White-type cell adjusted for 32 transits to provide an absorption path length of 55.1(2) m. The reader is referred to Ref. [11] for a more complete description of the recordings. Using a multiline fitting program, an empirical list of 12,254 lines with absolute intensities, was elaborated in the region and used to identify 2500 lines C_2H_4 with 5 ppm concentration in a high sensitivity CRDS study of acetylene [11]. The ethylene FTS list between 5800 and 6400 cm^{-1} is provided as Supplementary Material and displayed in Fig. 1. Line intensities at 294 K range between 1×10^{-24} and 6×10^{-22} cm/molecule.

2.2. Variational line list

Seven years ago, comprehensive ethylene line lists were obtained in Ref. [10] from extensive first-principle calculations using accurate *ab initio* potential and dipole moment surfaces (PES [12] and DMS [13], respectively). Lists at $T = 80$, 160, and 296 K were elaborated in the 0–6400 cm^{-1} region while in the range 0–5200 cm^{-1}, line lists were calculated at 500 and 700 K. These lists are accessible at http://theorets.univ-reims.fr and http://theorets.tsu.ru web sites. Very recently, the calculations at 130 K and 296 K were extended up to 9000 cm^{-1} using the same PES and DMS [9]. The resulting variational lists are provided as Supplementary Material of Ref. [9]. Note that the intensity cutoff was fixed to 1×10^{-25} cm/molecule which is a factor of 10 below the smallest intensity values of the experimental list under analysis.

2.3. Assignment procedure

The birds-eye comparison displayed in Fig. 1 illustrates the overall good agreement between the variational and experimental lists for the whole studied region. Nevertheless, at a larger scale (Fig. 2), a one-to-one correspondence between the experimental and calculated transitions is not straightforward. The uncertainties on the variational positions and intensities combined with a high spectral congestion make rovibrational assignments based exclusively on the agreement between experiment and theory, hazardous (about 500 band centers are calculated in the 5800–6200 cm^{-1}, most of them being not properly converged). The LSCD relations provide a strict criterion to validate the assignments, in particular when the experimental uncertainty on the line positions is small (typically 1×10^{-3} cm^{-1}, in our case). Let us recall that LSCD relations are fulfilled for a pair of transitions when the upper state energy values derived from the two measured transition frequencies are identical (within the measurement uncertainty, thus about within 2×10^{-3} cm^{-1}). The upper state energy of an assigned transition is simply obtained by adding the lower state energy value provided by variational line list to the measured transition wavenumber.

The assignment procedure consisted in considering separately the different bands in decreasing order of their intensities, thus starting from the $\nu_5 + \nu_9$ band around 6150 cm^{-1}. Then, for each strong line of the experimental list (ExpL), we identified the most probable counterpart in the calculated list (VarL). Using the rovibrational assignment provided

Table 1
Statistics of transitions assigned to five bands in the absorption spectrum of $^{12}C_2H_4$ between 5868 and 6219 cm^{-1} and comparison of the measured and calculated band intensities.

Band	Variational [9] [a]			Assigned lines				
	Band center [b] (cm^{-1})	Nb.	Int. sum (cm/molecule)	Nb.	Int. sum (cm/molecule)			
					Exp.	Var.	Exp./Var.	
$\nu_2+\nu_3+\nu_{11}$	5916.94202	1692	1.31×10^{-20}	247	8.36×10^{-21}	6.22×10^{-21}	1.34	
$\nu_2+\nu_6+\nu_9$	5925.74423	1556	1.17×10^{-20}	38	2.39×10^{-21}	1.39×10^{-21}	1.72	
$\nu_1+\nu_{11}$	5948.75370	1247	1.01×10^{-20}	134	5.58×10^{-21}	3.70×10^{-21}	1.51	
$\nu_5+\nu_{11}$	5989.09283	2805	4.77×10^{-20}	597	3.60×10^{-20}	2.75×10^{-20}	1.31	
$\nu_5+\nu_9$	6149.15190	2703	7.76×10^{-20}	658	7.68×10^{-20}	5.77×10^{-20}	1.33	
		10,003	$\mathbf{1.60\times10^{-19}}$	**1674**	$\mathbf{1.29\times10^{-19}}$	$\mathbf{9.65\times10^{-20}}$	**1.37**	**Total**

Note.
[a] The intensity cutoff of the variational line list is 1×10^{-25} cm/molecule at 296 K [9].
[b] Variational position of the P transition reaching the $J=0$ level of the upper vibrational state.

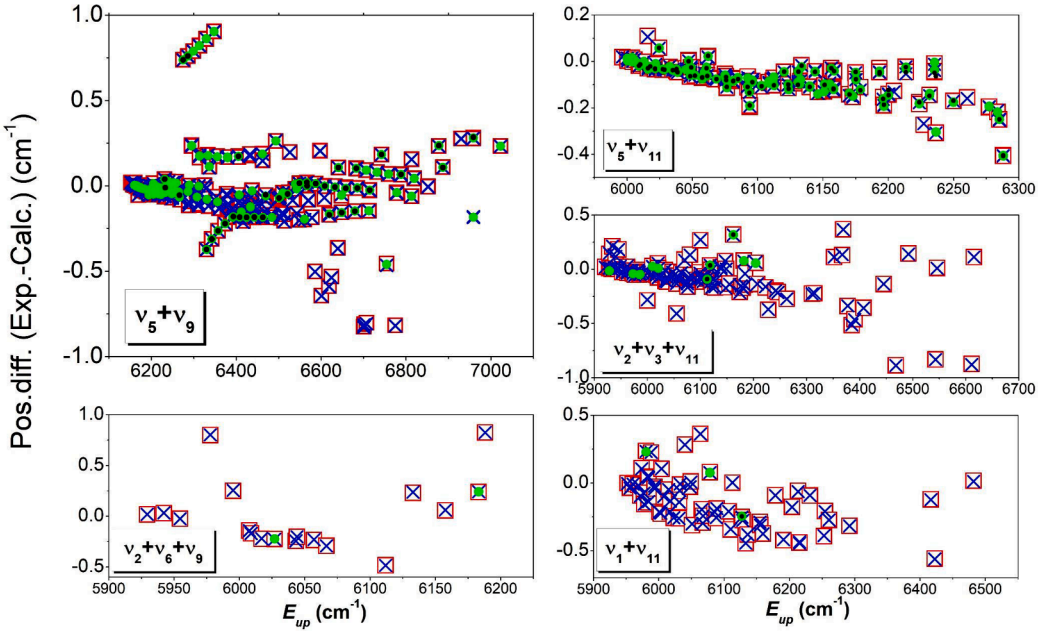

Fig. 4. Differences between the measured and variational line positions *versus* the energy of the upper state for the $^{12}C_2H_4$ transitions assigned in the 5868–6219 cm^{-1} interval. Each upper energy has various experimental determinations illustrated by the superposition of different symbols. Up to six transitions allowed for the determinations of some levels (for clarity, we limited to four the number of superimposed symbols).

in the calculated list [9], the other calculated transitions reaching the same upper level were extracted from the calculated list. Their position was shifted according to the (ExpL- VarL) position difference. The resulting variational lines with corrected positions were thus searched in the experimental list. In case of position agreement within $2–3\times10^{-3}$ cm^{-1} (LSCD criterion) and reasonable intensity agreement (a factor of two), the VarL assignment was considered as validated and the different lines sharing the VarL upper state were assigned.

Then, all the calculated transitions reaching the VarL upper state (including those without experimental counterpart) were removed from the variational list and we proceeded with the next strong experimental line. The procedure was found very efficient to assign most of the strong lines (see Fig. 3, where the assignments of the three strongest bands - $\nu_2+\nu_3+\nu_{11}$, $\nu_5+\nu_{11}$ and $\nu_5+\nu_9$- are highlighted). Note that we examined in details the few cases for which part of the assignments were validated by LSCD relations while a strong line involved in LSCD relations was absent in the experimental list.

After assignment of the three strongest bands, we considered the next dominant bands ($\nu_2+\nu_6+\nu_9$, $\nu_1+\nu_{11}$, $\nu_9+2\nu_{12}$ and $\nu_1+\nu_2+\nu_{12}$) for comparison to the set of unassigned lines of the experimental list. Although these bands have a similar intensity, we were able to assign transitions of the two first ones, only. Indeed, the assignments become more difficult for weak bands due to the increased density of lines and thus larger number of possible candidates to be associated to a given calculated transition, to the absence of some experimental lines which are obscured by stronger lines (and thus preventing the validation by LSCD relations) and the decreased accuracy of calculations for combination bands.

The statistics of the assignments of the five bands identified are summarized in Table 1. Overall a total of 1674 transitions could be assigned between 5868 and 6219 cm^{-1}. The list of the assigned transitions are provided as a separated Supplementary Material which includes the experimental positions and intensities, the corresponding calculated transitions from Ref. [9] providing the rovibrational assignments and a comparison to the positions and assignments of Ref. [8] (see below).

In Fig. 4, the deviations between the variational and experimental line positions are plotted *versus* the energy of the upper state obtained by adding the lower state energy value to the measured transition wavenumber. As all upper states energy levels are involved in LSCD relations, various energy determinations are available for each level. In the case of

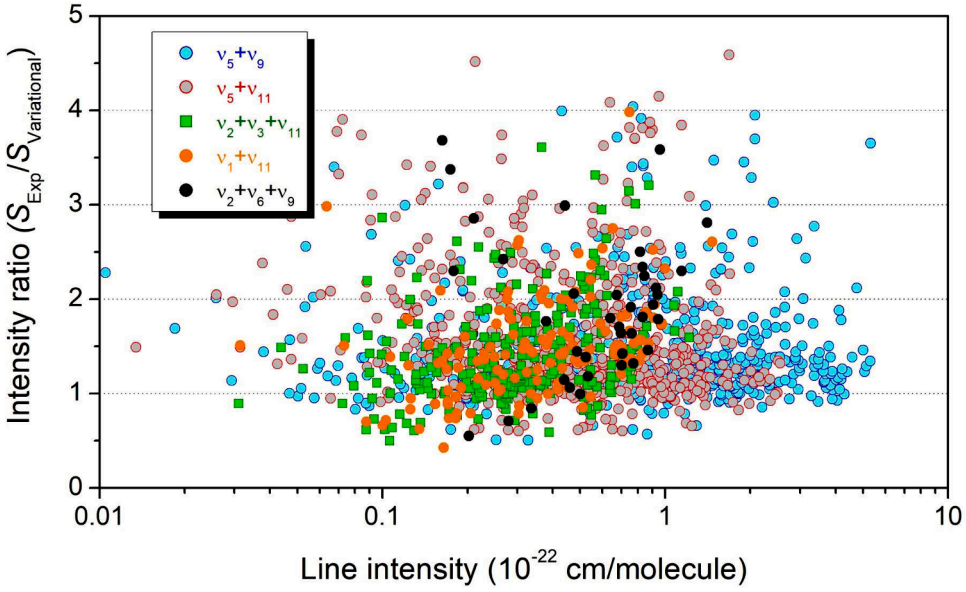

Fig. 5. Band-by-band intensity ratios for the five $^{12}C_2H_4$ bands assigned in the 5868–6219 cm^{-1} interval.

the two strongest bands, $\nu_5+\nu_{11}$ and $\nu_5+\nu_9$, LSCD relations were generally validated by four transitions involving the *P, Q* and *R* branches. In a few cases, up to six transitions were found to share the same upper state (for clarity, in Fig. 4, we have limited to 4 the number of superimposed symbols corresponding to distinct upper level determinations). Excluding a limited number of outliers, the general behavior of the deviations is similar for the five considered bands. The calculations agree very well with the measurements for the first rotational levels and then have the tendency to overestimate the upper state rotational energy (except for the $\nu_5+\nu_9$ band), the amplitude of the deviations increasing roughly linearly with the rotational energies up to values on the order of 0.5 cm^{-1} for rotational energies of 400 cm^{-1}. Similar rotational dependence of the deviations was evidenced in the 6700–7260 cm^{-1} [9] and interpreted as an incomplete convergence of the variational calculations when *J* increases. Let us note that, in the present work around 6000 cm^{-1}, global vibrational shifts are very small, less than 0.05 cm^{-1} for all the bands while, around 7000 cm^{-1}, vibrational shifts were found to range between −2.5 and 3.5 cm^{-1}.

3. Discussion

3.1. Intensity considerations

According to Table 1, the sum of the variational intensities of the assigned transitions of the five identified bands (9.65×10^{-20} cm/molecule) is smaller than measured (1.29×10^{-19} cm/molecule). The line-by-line intensity ratios plotted in Fig. 5 show a large dispersion with no systematic trends but on average, the underestimation of the calculated intensities is general for all the considered bands (the band intensity ratios range between 1.31 and 1.72 – see Table 1). The line-by-line variation of the intensity ratios is larger than the uncertainty on the experimental intensity values (a few % for non-too weak isolated lines). Inaccuracies of the

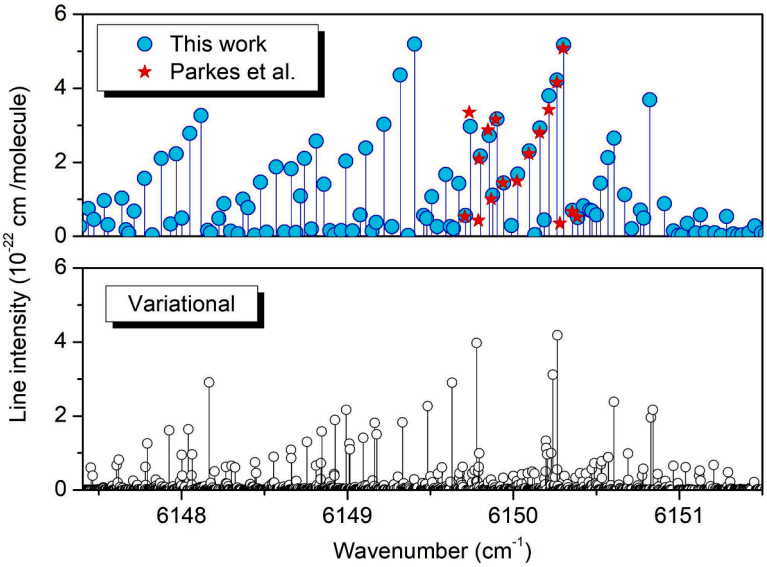

Fig. 6. Comparison of experimental and variational line lists of ethylene in the region of the $^{Q}Q_4$ transitions of the $\nu_5+\nu_9$ band. On the upper panel, the FTS line list analyzed in this work (blue circles) is superimposed to the CRDS line list obtained by Parkes et al. [7] (red stars). For a proper comparison of these stick spectra, variational doublets have been merged in single transitions with the sum of the intensity of the two components.

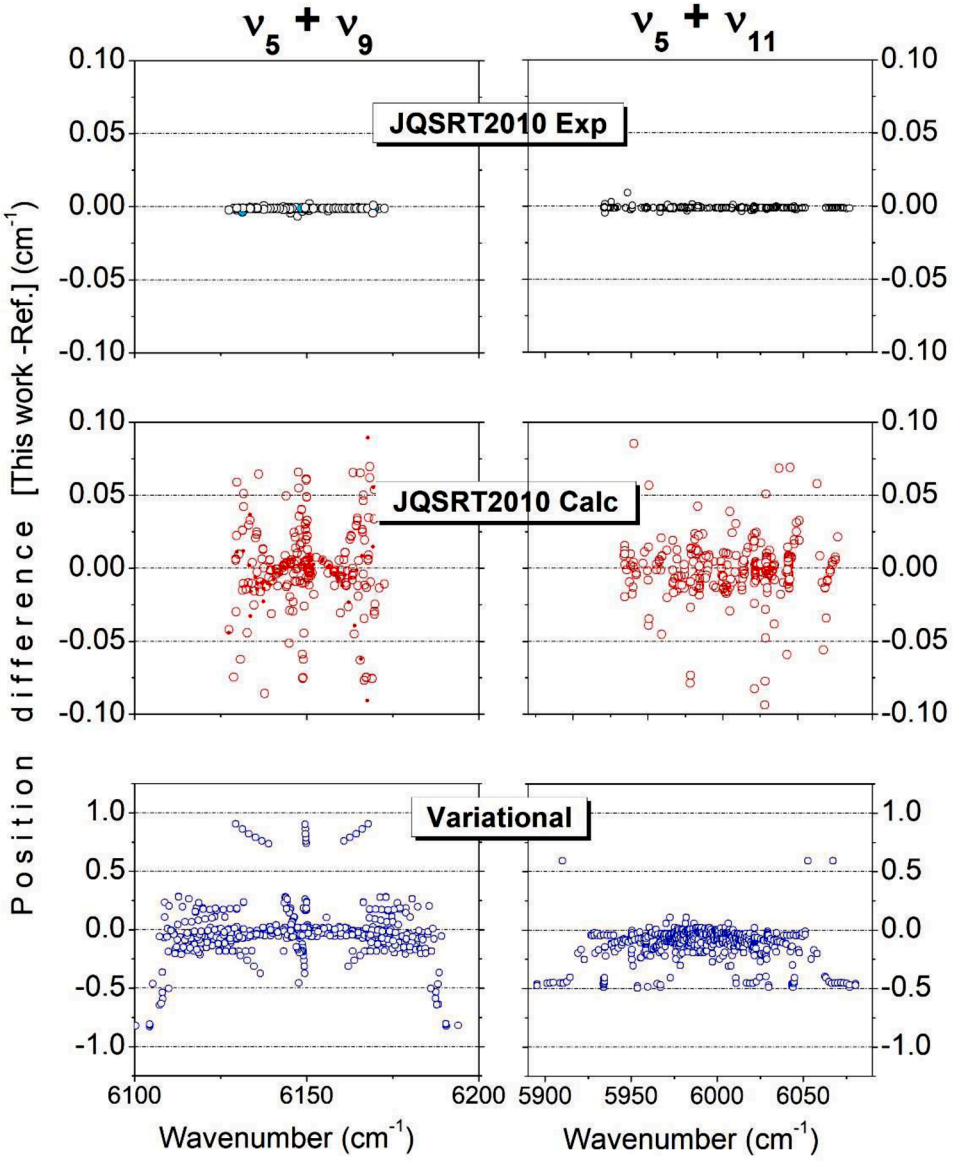

Fig. 7. Position comparison for the $\nu_5+\nu_9$ and $\nu_5+\nu_{11}$ bands of ethylene. Our measured position values are compared to the experimental and calculated values by Loroño Gonzalez et al. [8] (upper and middle panels, respectively) and to the variational values of Ref. [9] (lower panel). Note the different scale used for the lower panels.

variational intensities may be due to the low-order (order 4) of the normal-mode expansion used for the dipole moment, to the lack of convergence of the high J energy levels and/or to the numerous possible local resonances between the observed bright states and the nearby dark states. The overview comparison of Fig. 1 shows that the calculated spectrum has a more regular appearance than the observed spectrum. Let us note that the sum of the variational intensities of the assigned transitions represents about 60 % of the total of the variational intensities of the transitions calculated in the region.

As mentioned in the introduction, the only previous intensity information available in the region is due to Parkes et al. [7] who studied 17 strong $^{Q}Q_4$ lines of the $\nu_5+\nu_9$ band by cavity ring down spectroscopy near 6150 cm^{-1}. The measurement of the large line intensities of the considered transitions by the highly sensitive CRDS technique required to decrease the ethylene concentration in the gas sample. CRDS recordings were performed with 2 % ethylene in argon at a total pressure limited to 120 mTorr. In addition, series of recordings of ethylene broadened by air was performed to evaluate the impact of the pressure line broadening on the detection limit of ethylene in the atmosphere [7].

In Fig. 6, the CRDS line list [7] is superimposed to the present FTS line list and compared to the variational calculations [9]. Considering the quite different experimental conditions used for the FTS and CRDS recordings (pure ethylene at 0.36 Torr in our work and 2 % ethylene in argon at a total of 120 mTorr, in Ref. [7]), the agreement between the experimental intensities is very satisfactory. The CRDS line positions appear to be underestimated by values up to 5×10^{-3} cm^{-1}. In the considered region, the quality of the variational calculations is not optimum in particular for line intensities (Fig. 6).

3.2. *Line position comparison to the results of Ref. [8]*

In Ref. [8], Loroño Gonzalez et al. reported an analysis of ethylene room temperature spectra recorded by FTS and diode laser opto-acoustic spectroscopy between 6030 and 6250 cm^{-1}. A set of 608 transitions of the $\nu_5+\nu_9$ and $\nu_5+\nu_{11}$ bands was rovibrationally assigned and modeled using an effective Hamiltonian model limited to the two interacting vibrational bands. Overall, the 608 assigned transitions involve 342 upper state energies (for comparison, in the present work, 607 upper

Table 2
Comparison of the amount of transitions and assignments for $^{12}C_2H_4$ between transitions, reported in this work and in Ref. [8].

	Loroño Gonzalez et al. *[8]*	*This work*
Spectral interval (cm^{-1})	5934.1–6172.7	5800–6400
Number of lines	608	12,254
Number of assignments	608 [a]	1674
Number of energy levels	342	607

Note.
[a] Including 502 assignments confirmed by LSCD relations, 30 assignments corrected and 76 assignments which could not be confirmed by LSCD.

state energies were determined from 1674 assigned transitions). The experimental list of Ref. [8] is limited to the positions of the 608 assigned transitions which are provided without line intensities.

We present in Fig. 7, a position comparison for the $\nu_5+\nu_9$ and $\nu_5+\nu_{11}$ bands between our values and the experimental and calculated position values reported by Loroño Gonzalez et al. The agreement between the experimental values is satisfactory with nevertheless a systematic shift between the two datasets of about 1.3×10^{-3} cm^{-1}. In the case of the positions calculated using the effective Hamiltonian developed in Ref. [8], the dispersion is much larger with some systematic trends for some series of transitions, indicating that the developed model does not reach the experimental accuracy. This is probably related to the limitation of the effective Hamiltonian to two interacting states while several dark states located in the region may interact with the two observed bright states. We have added in Fig. 7, the position differences with the variational calculations which show a mostly symmetric appearance as identical deviations are observed in the *P* and *R* branches (due to LSCD relations).

As concerns rovibrational assignments, more than 502 of the 608 assignments proposed by Loroño Gonzalez et al. [8] are presently validated. Among the remaining assignments, about 30 had to be corrected and 76 could not be validated using LSCD relations (see Table 2). Note that different conventions for the axis system and D_{2h} character table exist in the literature for C_2H_4 (see Refs. [6,8,14-16]), leading to different symmetry labels of the vibrational modes. In order to properly compare our assignments with those of Loroño Gonzalez et al. [8], the B2 and B3 symmetry labels have to be switched. The line-by-line comparison to Ref. [8] is included in the list of assigned transitions provided as Supplementary Material.

Finally, a comment deserves to be given about the application of the LSCD relations based on the variational values of the lower state energies, E''_{var} [9]. In the present work, the five assigned bands are cold bands. The comparison of the ground state E''_{var} values to their HITRAN counterparts [1], E''_{HITRAN} shows a very good agreement: up to rotational energies around 600 cm^{-1} (which corresponds to the highest E'' values of our assigned transitions), the ($E''_{var}-E''_{HITRAN}$) differences have an average value on the order of 2×10^{-3} cm^{-1} with an RMS on the order of 3×10^{-3} cm^{-1}, excluding a series of a few levels showing deviations up to 0.03 cm^{-1}. Using both the HITRAN and the variational lower state energies, the upper state energies (E') of the assigned transitions were calculated. Overall, the RMS values of the E' determinations were found significantly better using E''_{HITRAN} instead of E''_{var} from Ref. [9] (average RMS values of about 1.3×10^{-3} cm^{-1} and 2.0×10^{-3} cm^{-1}, respectively). In other words, the use of E''_{HITRAN} instead of E''_{var} leads to a better coincidence of the various determinations of the upper state energies and the LSCD relations are better fulfilled. For future analysis using the LSCD relations, we thus recommend to substitute the corresponding HITRAN values to the ground state energy values of the variational list of Ref. [9].

3.3. Comparison to the ExoMol line list

The ExoMol calculated line list is an alternative variational list

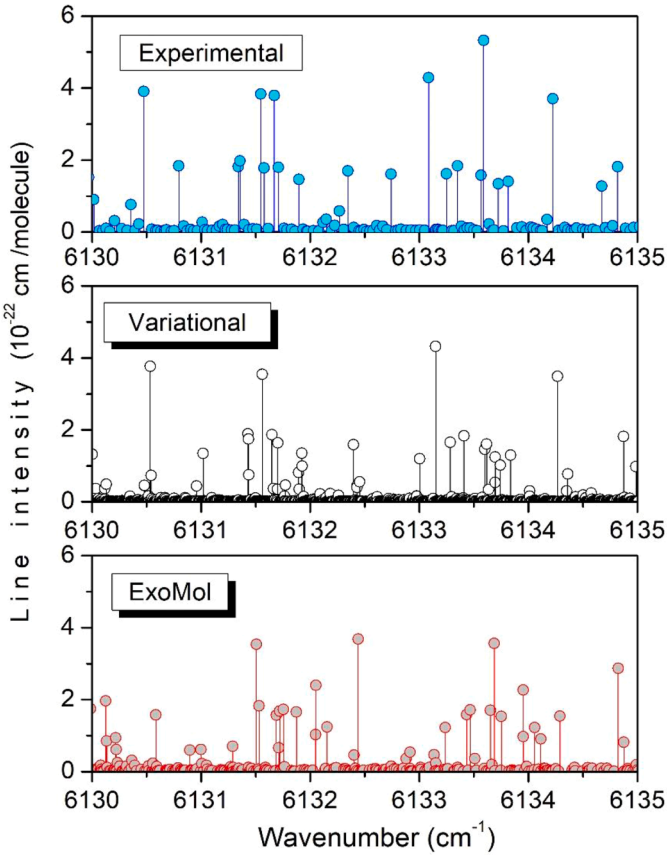

Fig. 8. Comparison of the experimental list of ethylene at 296 K to the variational list of Ref. [9] and to the ExoMol calculated lists [17,18]. For a proper comparison of these stick spectra, variational doublets have been merged in single transitions with the intensity sum of the two components.

available up to 7000 cm^{-1} [17,18] which can also be used to assign the ethylene spectrum. In Ref. [9], we presented some comparisons around 6800 cm^{-1} showing significant deviations between our variational lists and the ExoMol lists, both showing important differences compared to the experimental spectra. In the present region at lower energy, the bird-eye comparison at the scale of Fig. 1 shows a similar level of agreement for both calculations compared to experiment. At a larger scale as that adopted for Fig. 8, the one-to-one correspondence between experimental lines and calculated transitions is not straightforward for none of the two calculations, although the position agreement with experiment seems to be slightly better for our variational calculations [9]. Let us mention, that due to different choices in the vibrational labeling (ExoMol labeling uses local mode quantum numbers [17]), a direct comparison of the two calculated line list is not easy.

4. Conclusion

The line list attached to the present work is the first extensive line list released with absolute line intensities in the region of the first overtone of the CH stretching manifold (5800–6400 cm^{-1}). This strong absorption interval is of potential interest for ethylene monitoring. The quality of recent variational calculations [9] combined with the systematic use of LSCD relations has been found sufficient to significantly enlarge the set of assignments available in the region. About 1700 transitions were assigned to five bands while previous assignments were limited to about 600 transitions of the two strongest bands [8]. The intensity sum of the assigned transitions represents about 60% of the total absorption in the region. On the basis of the obtained experimental information, an effective Hamiltonian modeling of the spectrum will be undertaken in

the region, including the five observed bright states and possible dark states predicted by theory [9]. To this end, the construction of an effective Hamiltonian and dipole moment operators, as proposed in Ref. [19], will be undoubtedly of great help. Finally, an improvement of the accuracy of both variational line positions and line intensities seems reachable using *(i)* higher order normal-mode expansions of the PES and DMS and *(ii)* a better suited basis set, compared to the model used in Refs. [9,10].

CRediT authorship contribution statement

O. Ben Fathallah: Investigation. **M. Rey:** Investigation. **A. Campargue:** Investigation.

Declaration of competing interest

The authors declare that they have no known competing financial interests or personal relationships that could have appeared to influence the work reported in this paper.

Acknowledgements

Jean Vander Auwera (Université Libre de Bruxelles) is acknowledged for the recording of the FTS spectrum of ethylene. This project is supported by the Agence Nationale de la Recherche (e_PYTHEAS ANR-16-CE31–0005 and ANR-RNF TEMMEX-ANR-21–3 CE 0–0053–01). H. Aroui (ENSIT, Tunis) is acknowledged for a careful reading of the manuscript. MR acknowledges support from the Romeo computer center of Reims Champagne-Ardenne.

Supplementary materials

Supplementary material associated with this article can be found, in the online version, at doi:10.1016/j.jqsrt.2024.108905.

References

[1] Gordon IE, Rothman LS, Hargreaves RJ, Hashemi R, Karlovets EV, Skinner FM, et al. The HITRAN2020 molecular spectroscopic database. J Quant Spectrosc Radiat Transf 2022;277:107949. https://doi.org/10.1016/j.jqsrt.2021.107949.

[2] Boschetti A, Bassi D, Iacob E, Iannotta S, Ricci L, Scotoni M. Resonant photoacoustic simultaneous detection of methane and ethylene by means of a 1.63-μm diode laser. Appl Phys B 2002;74:273–8. https://doi.org/10.1007/s003400200790.

[3] Rossi A, Buffa R, Scotony M, Bassi D, Iannotta S, Boschetti A. Optical enhancement of diode laser-photoacoustic trace gas detection by means of external Fabry–Perot cavity. Appl Phys Lett 2005;87:041110. https://doi.org/10.1063/1.2000341.

[4] Bach M, Georges R, Herman M, Perrin A. Investigation of the fine structure in overtone absorption bands of $^{12}C_2H_4$. Mol Phys 1999;97:265–77. https://doi.org/10.1080/00268979909482828.

[5] Platz T, Demtroder W. Sub-doppler optothermal overtone spectroscopy of ethylene and dichloroethylene. Chem Phys Lett 1998;294(4–5):397–405. https://doi.org/10.1016/S0009-2614(98)00885-9.

[6] Kapitanov VA, YuN Ponomarev. High resolution ethylene absorption spectrum between 6035 and 6210 cm^{-1}. Appl Phys B 2008;90:235–41. https://doi.org/10.1007/s00340-007-2920-3.

[7] Parkes AM, Lindley RE, Orr-Ewing AJ. Absorption cross-sections and pressure broadening of rotational lines in the $\nu_5+\nu_9$ band of ethane measured by diode laser cavity ring down spectroscopy. Phys Chem Chem Phys 2004;6:5313–7. https://doi.org/10.1039/B413238F.

[8] Loroño Gonzalez MA, Boudon V, Loëte M, Rotger M, Bourgeois MT, Didriche K, Herman M, Kapitanov VA, YuN Ponomarev, Solodov AA, Solodov AM, Petrova TM. High-resolution spectroscopy and preliminary global analysis of C–H stretching vibrations of C_2H_4 in the 3000 and 6000 cm^{-1} regions. J Quant Spectrosc Radiat Transf 2010;111:2265–78. https://doi.org/10.1016/j.jqsrt.2010.04.010.

[9] Mraidi S, Manceron L, Rey M, Aroui H, Campargue A. High resolution spectroscopy and a theoretical line list of ethylene between 5000 and 9000 cm^{-1}. J Quant Spectrosc Radiat Transf 2023;310:108734. https://doi.org/10.1016/j.jqsrt.2023.108734.

[10] Rey M, Delahaye T, Nikitin AV, Tyuterev VG. First theoretical global line lists of ethylene ($^{12}C_2H_4$) spectra for the temperature range 50–700 K in the far- infrared for quantification of absorption and emission in planetary atmospheres. Astron Astrophys 2016;594:A47. https://doi.org/10.1051/0 0 04-6361/201629004.

[11] Lyulin OM, Mondelain D, Béguier S, Kassi S, Vander Auwera J, Campargue A. High sensitivity absorption spectroscopy of acetylene by CRDS between 5851 and 6341 cm^{-1}. Mol Phys 2014;112:2433–44. https://doi.org/10.1080/00268976.2014.906677.

[12] Delahaye T, Nikitin AV, Rey M, Szalay PG, VlG Tyuterev. A new accurate ground-state potential energy surface of ethylene and predictions for rotational and vibrational energy levels. J Chem Phys 2014;141:104301. https://doi.org/10.1063/1.4894419.

[13] Delahaye T, Nikitin AV, Rey M, Szalay PG, VlG Tyuterev. Accurate 12D dipole moment surfaces of ethylene. J Chem Phys 2015;639:275–82. https://doi.org/10.1016/j.cplett.2015.09.042.

[14] Lafferty WJ, Flaud JM, Kwabia Tchana F. The high–resolution infrared spectrum of ethylene in the 1800–2350 cm^{-1} spectral region. Mol Phys 2011;109:2501–10. https://doi.org/10.1080/00268976.2011.577040.

[15] Sanzharov M, Rotger M, Wenger M, Loëte M, Boudon V, Rouzée A. D2hTDS-ST software for Stark spectrum simulation of X2Y4 asymmetric-top molecules. J Quant Spectrosc Radiat Transf 2011;112:41–52. https://doi.org/10.1016/j.jqsrt.2010.08.023.

[16] Wenger C, Raballand W, Rotger M, Boudon V. D2h top data system (D2hTDS) software forspectrum simulation of X2Y4 asymmetric molecules. J Quant Spectrosc Radiat Trans 2005;95:521–38.

[17] Mant BP, Yachmenev A, Tennyson J, Yurchenko SN. ExoMol molecular line lists - XXVII: spectra of C_2H_4. Month Not R Astronom Soc 2018;478:3220–32.

[18] Tennyson J, et al. The ExoMol database: Molecular line lists for exoplanet and other hot atmospheres. J Mol Spectrosc 2016;327:73–94. https://doi.org/10.1016/j.jms.2016.05.002.

[19] Rey M. Novel methodology for systematically constructing global effective models from ab initio-based surfaces:a new insight into high-resolution molecular spectra analysis. J Chem Phys 2022;156:224103. https://doi.org/10.1063/5.0089097.